Nonlinear optical contrast enhancement in OCT

Claudio Vinegoni, Jeremy S. Bredfeldt, and Dan L. Marks
Beckman Institute for Advanced Science and Technology, University of Illinois at Urbana-Champaign

Stephen A. Boppart
Department of Electrical and Computer Engineering, Beckman Institute for Advanced Science and Technology, Bioengineering Program, College of Medicine, University of Illinois at Urbana-Champaign, 405 North Mathews Avenue, Urbana, Illinois 61801
boppart@uiuc.edu

Abstract: We report on a new interferometric technique for measuring Coherent Anti-Stokes Raman Scattering and Second Harmonic Generation signals. The exploitation of these optical nonlinearities for molecular contrast enhancement in Optical Coherence Tomography is presented.

OCIS codes: (111.4500) Optical coherence tomography; (300.6230) Spectroscopy, coherent anti-Stokes Raman scattering; (190.4410) Nonlinear optics, parametric processes; (120.3180) Interferometry; (040.2840) Heterodyne; (190.4160) Multiharmonic generation.

1. Introduction

Optical Coherence Tomography (OCT) is an interferometric optical imaging technique capable of imaging tissue microstructure at near histological resolutions [1]. A serious drawback of this technique is that the linear scattering properties of pathological tissue probed by OCT are often morphologically and/or optically similar to the scattering properties of normal tissue. This implies a need for the development of novel contrast mechanisms for OCT. Possible methods that have been recently developed are spectroscopic OCT [2], pump and probe technique [3], and the use of engineered microspheres [4] or microbubbles [5]. Unfortunately most of these methods require the presence of a contrast agent, which can modify the biology under investigation.

In this paper we propose and present a new method to achieve enhanced OCT contrast, exploiting optical nonlinearities. The nonlinear effects addressed in this work are in particular Coherent Anti-Stokes Raman Scattering (CARS) and Second Harmonic Generation (SHG). This method can additionally be extended for Third Harmonic Generation (THG), Coherent Stokes Raman Scattering (CSRS) microscopy, and other coherent scattering processes.

2. CARS contrast enhancement

In recent years CARS has been successfully employed to provide vibrational contrast in scanning microscopy [6]. In CARS spectroscopy, the frequencies of two incident lasers, ν_p (pump) and ν_s (Stokes), are chosen such that the difference $\nu_p - \nu_s = \nu_v$ is equal to a Raman-active vibrational mode of the molecule under study. In opposition to Raman spectroscopy, CARS is a non-linear, four-wave mixing χ^3 process. The CARS field is therefore a result of the interaction between four photons and is generated in the phase-matching direction at the anti-Stokes frequency $\nu_{AS} = 2\nu_p - \nu_s$, with the CARS signal intensity being linearly dependent on the Stokes field intensity and quadratically dependent on the pump field intensity. The main advantage of this kind of spectroscopy is that the vibrational contrast is inherent to the chemical species, and does not require natural of artificial contrast agents [7]. To note that in all the CARS microscopy techniques, the anti-Stokes photons are counted in order to estimate the density of the Raman scatterers and/or the Raman susceptibility magnitude in the focal volume of the microscope. This implies a loss of the spectral phase information. The new CARS interferometric technique that we present here allows heterodyne detection and the possibility to obtain a full reconstruction of the magnitude and phase of the sample Raman susceptibility [8,9].

The CARS interferometer is schematically shown in Fig. 1(a). An excitation field consisting of two pulses centered at the pump and Stokes wavelengths is divided by a beamsplitter into two separate interferometer paths referred to as the “sample arm” and the “reference arm”. Unique to the general methodology of our technique, a reference sample of a molecule is placed in the “reference arm” (sample R), in addition to the sample under investigation placed in the “sample arm” (sample S). If the frequency difference between pump and Stokes pulses is tuned to a Raman active vibrational mode present in both sample S and sample R, an anti-Stokes signal is generated in each arm of the interferometer [9]. Because the anti-Stokes pulse phase is deterministically related to the phase of the pump and the Stokes pulses, the anti-Stokes fields are coherent with the excitation fields and also with each other. When these anti-Stokes fields are temporally and spatially overlapped, interference can be observed [9].

In our experiment, the pump and Stokes pulses, are tuned at 807 nm and 1072 nm respectively, in order to excite the strong isolated Raman-active vibrational mode of benzene at 3063 cm^{-1}. The anti-Stokes signals generated in

each arm are collected in the collinear phase matching direction. The relative delay is scanned by a computer-controlled single axis translation stage at a constant rate in the reference arm, and the CARS signal intensity is measured with a photomultiplier tube (PMT).

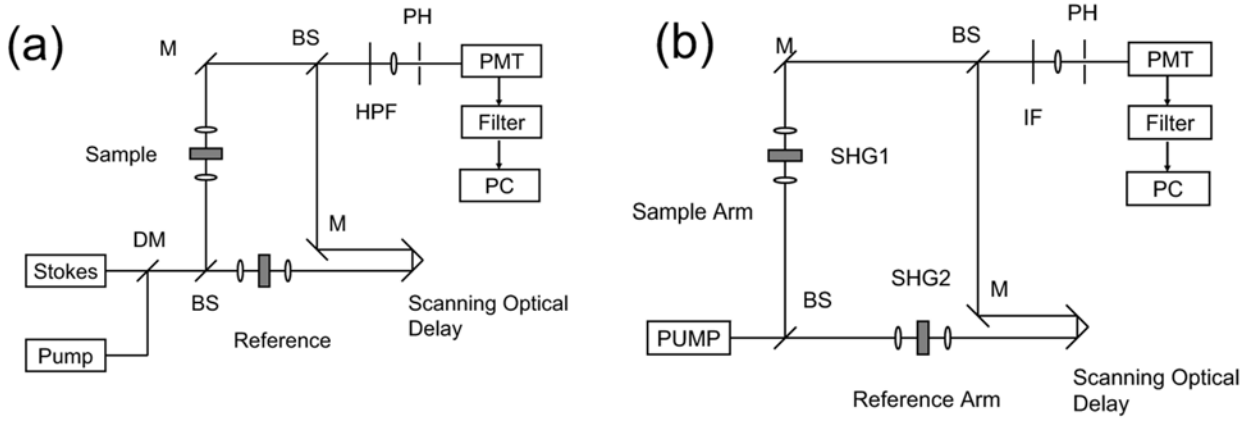

Fig.1. (a) Setup of the interferometric CARS measurement system. Benzene was used for both the reference and the sample molecular species. DM, dichroic mirror; BS, beamsplitter; M, mirror; HPF, high-pass-filter; PH, pin-hole. (b) Setup of the interferometric SHG measurement system. Two different nonlinear crystals (Type I) were used in the reference and in the sample arms respectively. IF, interference-filter.

After having proved the signal is true CARS resonance, interferograms were acquired. Fig.2(a) shows a measured interferogram resulting from the interference between the two anti-Stokes signals. The axial resolution of the interferometric CARS measurement technique, was found to be equal to 32 μm. This result indicates that two anti-Stokes signals generated in separate samples can be demodulated interferometrically, where the amplitude of the fringe envelope gives information about the concentration of the scatterers in the focal volume of the sample objective lens.

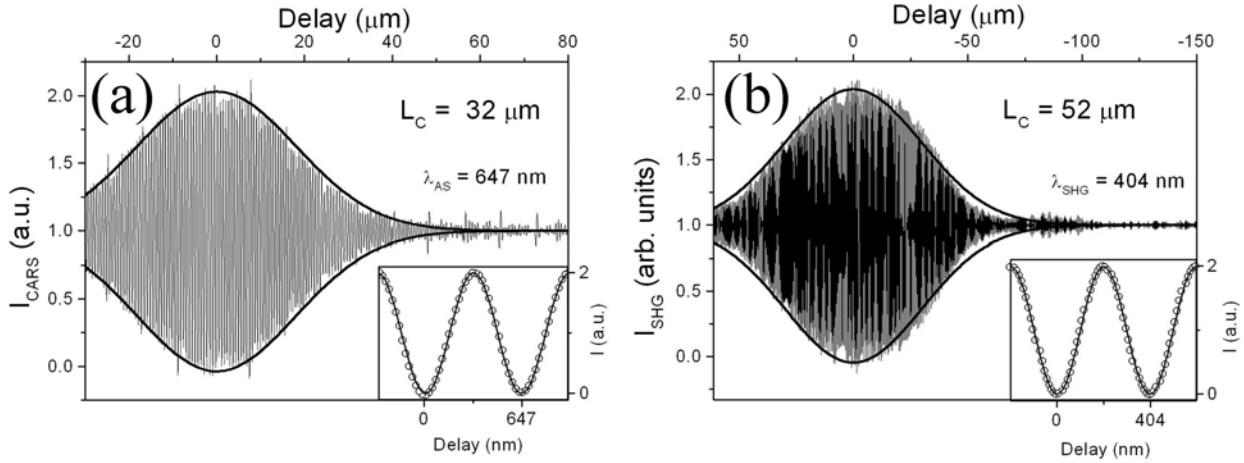

Fig.2. (a) CARS interferogram and (b) SHG interferogram detected at the beamsplitter BS of the setups shown in Fig.1. The interferogram is recorded as the pathlength of the reference arm R is scanned. The modulus of the degree of the coherence function is used to fit the envelope of the interferogram. In the inset is shown an enlarged version of the interference pattern and its fit by the real part of the degree of coherence function (open circles, experimental data; solid line, fit). L_c is the coherence length of the pulse. λ_{AS} (λ_{SHG}) is the wavelength of the CARS (SHG) signal.

The presence of interference clearly demonstrates the potential of CARS for providing molecular contrast for OCT-like interferometric imaging systems. In fact, the presence of the interference indicates that similar Raman-active vibrational frequencies are present in both the reference and the sample arm at the same path length from the detector. The "fingerprint" nature of Raman spectroscopy, combined with the possibility to switch between different samples R in the "reference arm", could thus permit selective detection and imaging, within the above mentioned axial resolution, of different molecular species present in the sample S under investigation [9].

3. SHG contrast enhancement

SHG, also known as frequency doubling, has recently emerged as a valid imaging contrast mechanism for microscopic imaging of cell and tissue structures and functions [10]. SHG, in opposition to CARS, is a χ^2 process in which two photons at the fundamental frequency are converted into a single photon at exactly twice the frequency without having any absorption and/or re-emission from the sample [11]. The main advantages of SHG microscopy are the high resolution typically achieved in nonlinear microscopy and its applications concerning the structure in live tissues of endogenous proteins such as collagen without the addition of exogenous labels [12].

The SHG interferometer is similar to the CARS interferometer and is shown in Fig. 1(b). In this configuration instead of having a Stokes and a Pump laser, only the Pump laser at 807 nm is present. In the "reference arm", a reference nonlinear crystal (Type I) is present in which SHG signal is created. In the "sample arm" a different kind of nonlinear crystal, always of Type I, is present. The signals generated in both the crystals are overlapped as in the CARS configuration scheme.

Fig.2(b) shows the measured interferogram resulting from the interference between the two SHG signals. This result indicates that two SHG signals generated in separate samples can be demodulated interferometrically. Even in this case the presence of interference clearly demonstrates the potential of SHG and resonance-enhanced SHG as a promising technique for providing molecular contrast for OCT-like interferometric imaging systems. The presence of a nonlinear crystal in the reference arm will allow one to interferometrically demodulate the SHG signal created in the sample under study present in the "sample arm".

4. Conclusions

In conclusion, we have described a novel technique for contrast enhancement in OCT based on optical nonlinearities. The contrast mechanism is based on resonant enhancement of the third order and second order nonlinear susceptibility of the molecules under investigation.

The interference between two CARS signals generated in separate samples (or alternatively two SHG signals), was observed allowing for heterodyne detection. This result is extremely promising for the development of a new molecular imaging technique (NIVI) based on non-linear, low-coherence interferometry [13]. In this work we focused on forward CARS and SHG, but epi-detected CARS and SHG are coherent as well, and are compatible with OCT coherence-ranging systems. CARS and SHG interferometry provide the advantages of interferometric detection and at the same time provide OCT with molecular-specific contrast. These advantages could make CARS and SHG interferometry a powerful tool for biological imaging with OCT. Moreover the same configuration scheme could be exploited for Third Harmonic Generation (THG), Coherent Stokes Raman Scattering (CSRS) microscopy, and other coherent scattering processes

5. References

[1] S. A. Boppart, B. E. Bouma, C. Pitris, J. F. Southern, M. E. Brezinski, and J. G. Fujimoto, "*In vivo* cellular optical coherence tomography imaging," Nature Medicine **4**, 861, (1998).

[2] U. Morgner, W. Drexler, F. X. Krtner, X. D. Li, C. Pitris, E. P. Ippen, and J. G. Fujimoto, "Spectroscopic optical coherence tomography," Opt. Lett. **25**, 111 (2000).

[3] K. D. Rao, M. A. Choma, S. Yazdanfar, A. M. Rollins, and J. A. Izatt, "Molecular contrast in optical coherence tomography by use of a pump-probe technique," Opt. Lett. **28**, 340 (2003).

[4] T. M. Lee, A. L. Oldenburg, S. Sitafalwalla, D. L. Marks, W. Luo, F. J. Toublan, K. S. Suslick, and S. A. Boppart, "Engineered microsphere contrast agents for optical coherence tomography," Opt. Lett. **28**, 1546 (2003).

[5] J. K. Barton, J. B. Hoying, and C. J. Sullivan, "Use of microbubbles as an optical coherence tomography contrast agent," Acad. Radiol. **9**, S52 (2002).

[6] A. Zumbusch, G. R. Holtom, and X. S. Xie, "Three-dimensional vibrational imaging by Coherent anti-Stokes Raman scattering," Phys. Rev. Lett. **82**, 4142 (1999).

[7] A. Volkmer, J. X. Cheng, and X. S. Xie, "Vibrational imaging with high sensitivity via epi-detected coherent anti-Stokes Raman scattering microscopy," Phys. Rev. Lett. **87**, 23901 (2001).

[8] D. L. Marks, J. Bredfeldt, S. Hambir, D. Dlott, B. Kitchell, M. Gruebele, and S. A. Boppart "Molecular species sensitive optical coherence tomography using coherent anti-Stokes Raman scattering spectroscopy," in Optical Eng. and Biomed. Optics, Proc. SPIE 4956 (2003).

[9] J. S. Bredfeldt, D. L. Marks, C. Vinegoni, S. Hambir, and S. A. Boppart, "Coherent anti-Stokes Raman scattering heterodyne interferometry" submitted (2003); E-print at arxiv.org/physics/0311057, http://www.arxiv.org/abs/physics/0311057.

[10] P. J. Campagnola, and L. M. Loew, "Second-harmonic imaging microscopy for visualizing biomolecular arrays in cells, tissues and organisms," Nature Biotech.. **21**, 1356 (2003).

[11] P. Stoller, P. M. Celliers, K.M. Reiser, and A. M. Rubenchik, "Quantitative second-harmonic generation microscopy in collagen", App. Opt. **42**, 5209 (2003).

[12] R. M. Brown, A. C. Millard, and P. J. Campagnola, "Macromolecular structure of cellulose studied by second-harmonic generation imaging microscopy," Opt. Lett., **28**, 2207 (2003).

[13] D. L. Marks and S. A. Boppart, "Nonlinear interferometric vibrational imaging: theory and simulation," submitted (2003); Eprint at arxiv.org/physics/0311071, http://www.arxiv.org/abs/physics/0311071.